Research on Engineering Structures & Materials
www.jresm.org
Research Group

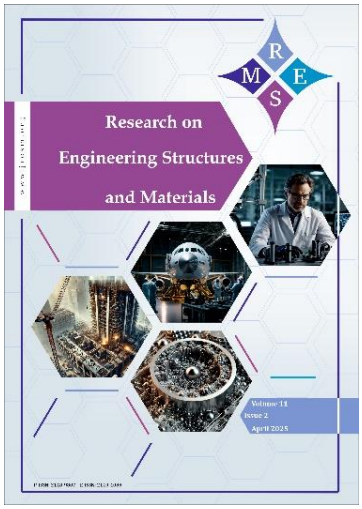

Seismic response assessment of RC frame buildings with masonry infill openings and soft story irregularity under dynamic soil–structure interaction

B R Shilpa, G Narayana, B K Narendra

Online Publication Date: 10 October 2026

URL: http://www.jresm.org/archive/resm2026-2353st0915rs.html
DOI: http://dx.doi.org/10.17515/resm2026-2353st0915rs

Journal Abbreviation: *Res. Eng. Struct. Mater.*

To cite this article
Shilpa B R, Narayana G, Narendra B K. Seismic response assessment of RC frame buildings with masonry infill openings and soft story irregularity under dynamic soil–structure interaction. *Res. Eng. Struct. Mater.*, 2026; 12(5): 4135-4152.

Disclaimer
All the opinions and statements expressed in the papers are on the responsibility of author(s) and are not to be regarded as those of the journal of Research on Engineering Structures and Materials (RESM) organization or related parties. The publishers make no warranty, explicit or implied, or make any representation with respect to the contents of any article will be complete or accurate or up to date. The accuracy of any instructions, equations, or other information should be independently verified. The publisher and related parties shall not be liable for any loss, actions, claims, proceedings, demand or costs or damages whatsoever or howsoever caused arising directly or indirectly in connection with use of the information given in the journal or related means.

Published articles are freely available to users under the terms of Creative Commons Attribution - NonCommercial 4.0 International Public License, as currently displayed at here (the “CC BY - NC”).

Research on Engineering Structures & Materials
www.jresm.org
MIM Research Group

Research Article

Seismic response assessment of RC frame buildings with masonry infill openings and soft story irregularity under dynamic soil–structure interaction

B R Shilpa [*,1,2,a], G Narayana [1,b], B K Narendra [3,c]

[1]*Department of Civil Engineering, S J C Institute of Technology, Chickballapur-562101, Karnataka, India and Visvesvaraya Technological University, Belagavi-590018, India*
[2]*Department of Civil Engineering, R R Institute of Technology, Bangalore 560090, Karnataka, India and Visvesvaraya Technological University, Belagavi-590018, India*
[3]*Department of Civil Engineering, Adichunchanagiri University, Mandya-571448,Karnataka India and Visvesvaraya Technological University, Belagavi-590018, India*

Article Info

Article History:

Received 15 Sep 2026
Accepted 02 Oct 2026

Keywords:

Dynamic soil–structure interaction;
Equivalent diagonal strut;
Inter-story drift ratio;
Masonry infill;
Opening percentage;
Reinforced concrete frame;
Soft story

Abstract

Masonry infill walls are widely used in reinforced concrete (RC) buildings, but their seismic behavior is often studied using fixed-base models without fully considering soil–structure interaction. This study investigates the seismic response of a ten-story, one-bay RC frame with 0%, 30%, and 50% infill openings, with and without a ground soft story, supported on four soil classes: soft soil, stiff soil, soft rock, and hard rock. The frame and infill walls were modeled in SAP2000 using equivalent diagonal compression struts, with reduced strut widths for openings. Soil–structure interaction was represented using a three-dimensional linear-elastic soil model directly connected to the isolated footings. Linear time-history analysis was carried out using the 2001 Bhuj earthquake record, scaled to a PGA of 0.1 g. The results show that soil conditions strongly affect the seismic response. The highest roof acceleration, about 2.7 g, occurred for regular infilled frames on stiff soil, while the largest roof displacement, about 241 mm, occurred for the fully infilled frame on soft soil. Soft-story frames showed higher ground-story drift, reaching about 1.2% on soft soil. Overall, the critical response varied with soil condition, indicating that fixed-base analysis may not always identify the governing case.

© 2026 MIM Research Group. All rights reserved.

1. Introduction

An earthquake releases stored energy along a fault, sending seismic waves to the surface that shake the ground, and any building on it. The building's inertia resists that motion, generating the internal forces engineers design against. Shaking severity depends on magnitude, distance, and, critically, soil type: soft soils amplify certain frequencies far more than rock, which is the core reason soil-structure interaction (SSI) matters. The 2001 Bhuj earthquake, used as the input record here, is a well-documented example of a high-magnitude event whose damage was worsened by local soil amplification. For buildings, severe inter-story drift can crack masonry infill, damage non-structural elements, and trigger a soft-story collapse mechanism, whereas one under-braced story absorbs nearly all the deformation, a pattern well documented in post-earthquake surveys [1-3]. Infill walls are usually treated as non-structural in design, even though they add real stiffness [4]. This is a limitation, since infill stiffens the frame and shortens its period substantially compared to a bare frame. The standard way to capture this without full finite element meshing is the equivalent diagonal strut, sized from the relative stiffness of panel and frame [4-6], refined recently through

*Corresponding author: shilpa.cv10@gmail.com
[a]orcid.org/0000-0003-1513-8523; [b]orcid.org/0009-0005-4226-6557; [c]orcid.org/0000-0002-9563-9717
DOI: http://dx.doi.org/10.17515/resm2026-2353st0915rs

cyclic testing [7, 8] and machine-learning-based prediction [9]. Openings reduce panel stiffness unevenly, and when irregular, can concentrate damage and help trigger soft-story behavior [1-3], in combination with other measures such as decoupled infill systems or buckling-restrained braces [10, 11]. Accordingly, the present study investigates bare, fully infilled, and 30%/50%-opening RC frames, each with and without a soft story, under different soil conditions considering dynamic soil-structure interaction.

1.1 Soil-Structure Interaction (SSI)

Conventional design assumes a rigid ("fixed") base. Real soil is flexible, so the building and soil respond as one coupled system [12]. Two mechanisms matter: kinematic interaction, where the foundation cannot perfectly track free-field ground motion, and inertial interaction, where the vibrating structure pushes back into the soil. Both lengthen the effective period and add radiation damping [12, 13]. Whether that helps or hurts depends on how the new period compares to the site's dominant period: a close match means resonance and amplification [14, 15]. The behavior/response-modification coefficient itself has also been shown to be sensitive to inertial soil–structure interaction [16], compounding the sensitivity to soil stiffness and building irregularity documented elsewhere [13, 17–23]. Findings across these studies remain fragmented [24], particularly for infilled frames whose stiffness, and therefore period, changes with infill openings and soft-story irregularity, which motivates the present paper.

1.2 Review of Related Literature

Beyond the strut-modeling and SSI studies discussed above, several recent works examine how infill layout, openings and soil flexibility interact. Amritha and Prasanth [25] modeled six- and eleven-story RC buildings with 0–40% infill openings together with the soil in a three-dimensional finite element model and found that soft soil increased roof displacement by up to about 21% and inter-story drift well beyond the fixed-base values, although soft-story irregularity was not varied. Messaoudi et al. [26] examined the effect of infill position and opening configuration on the seismic response of fixed-base RC frames, showing that both the location and the size of openings strongly influence story shear distribution and that removing infill from a story can raise its drift by up to 264%. Dias-Oliveira et al. [27] reviewed infilled-frame seismic behavior and highlighted that panel–frame interaction effects, beam–column joint detailing, and sliding shear failure of columns are frequently omitted from simplified infill models, leading to unconservative predictions. Zhang et al. [28] tested half-height infilled frames experimentally and found that the wall-to-column height ratio governs whether the frame column fails in bending or in shear, with the masonry material also affecting the degree of stiffness increase. Gamal et al. [29] studied the interaction between infill irregularity and dynamic response through modeling full-contact, gap and asymmetric infill configurations in moment resisting frames. They found that asymmetric infill placement induces torsional demands that are often ignored in design practice. Manojlovski et al. [30] presented a sliding flexible connection between infill panels and the bounding frame as a resilience method, which exhibited reduced damage to the panel-frame interaction compared to conventional tight-fit infill. Closer to the present scope, Karki et al. [31] evaluated a masonry-infilled RC frame under both fixed-base and soil-flexible conditions using the site classification of the revised Nepal building code, and found that soil-structure interaction altered the fundamental period, peak floor displacement, and inter-story drift ratio relative to the fixed-base case, though their study did not vary the infill opening ratio or soft-story configuration. Table I compares the most closely related studies in terms of structural model, infill modeling, opening ratios, soft-story conditions, soil classes and SSI modeling, and seismic input. Three limitations recur. First, stores that model openings and soft stores in detail [1, 26] assume a fixed base. Second, studies that model the soil explicitly [15, 25] consider a single soft deposit or two sand types, and do not vary soft-story presence together with the opening ratio. Third, the study that spans several code soil classes [31] uses static procedures, which cannot reproduce the frequency-dependent site and SSI amplification that controls floor accelerations. None of these studies combines infill opening ratio, soft-story irregularity and soil classes ranging from soft soil to hard rock within a single time-history framework with an explicit soil continuum, which is the gap addressed in this paper.

Table 1. Comparison of the present study with closely related studies

Study	Structure	Infill model	Openings	Soft story	Base / soil and SSI model	Analysis and input
Furtado et al. [1]	4-story RC frame	Double strut (macro-model)	16–65%	Yes	Fixed base	Modal, pushover, nonlinear dynamic (6 records)
Messaoudi et al. [26]	6-story, 3-bay RC frame	Single diagonal strut	10–90% (reduction factors)	Yes (15 layouts)	Fixed base	Numerical (OpenSees)
Amritha and Prasanth [25]	6- and 11-story, 3 × 3 bays	Plate micro-model and single strut	0–40%	Not varied	Two sands; direct 3D soil, hardening-soil model	Nonlinear time-history, Kobe 1995 scaled to 0.36 g
Santa-Ana-Lozada et al. [15]	Two irregular 10-story buildings	Infill in 3D FE model	Not varied	Vertical irregularity	Soft soil (EC8 type C); direct 3D nonlinear soil, viscous boundaries	Spectral, pushover, nonlinear time-history (42 records)
Karki et al. [31]	Masonry-infilled RC frame	Diagonal strut	Not varied	Not varied	NNBC 105:2020 soil types; flexible base	Linear static, pushover
Present study	10-story, one-bay RC frame	Diagonal strut with opening reduction	0, 30, 50%	With and without	Four classes (Vs = 175–2500 m/s); direct 3D linear-elastic soil	Linear time-history, Bhuj 2001

1.3 Choice of Analysis Method

Seismic demand can be estimated by equivalent static, response spectrum, nonlinear static (pushover) or time-history analysis [32]. Static and response spectrum methods rely on fixed-base design spectra and modal combination, so they cannot represent the frequency-dependent interaction between a soil column and the structure. Pushover analysis describes capacity and failure mechanisms but not dynamic amplification. Nonlinear time-history analysis is the most complete method, but it requires calibrated hysteretic models for the infill, the frame and the soil, and becomes very demanding for a three-dimensional soil continuum repeated for 7 configurations and 4 soil classes. Linear time-history analysis was therefore selected. It retains the full frequency content of the recorded motion and the coupled soil–structure dynamics, namely period lengthening, site amplification and radiation damping [33, 34], which are the effects under study, while keeping the parametric study tractable. Its limitations are that it cannot capture infill cracking, strut degradation, concrete yielding, soil nonlinearity or foundation uplift and sliding. The results are therefore elastic demand indicators, suitable for comparing configurations and soil classes, rather than predictions of damage.

1.4 Present Study

Building on this gap, the present study jointly varies infill opening percentage, soft-story irregularity and soil class within a single modeling framework, which prior studies [15, 25–31] have not done simultaneously. A one-bay, ten-story RC frame with seven configurations (bare frame; full infill, 30% and 50% openings, each with and without a ground soft story) is analyzed on

four IBC 2006 [35] site classes and on a fixed base, using the 2001 Bhuj earthquake record scaled to a PGA of 0.1 g. In this paper, the term "vulnerability ranking" is used only in a response-based sense: configurations are ranked by their peak roof displacement, peak floor acceleration and peak inter-story drift ratio (IDR). No damage states, fragility curves or probabilistic assessment are derived.

Within this definition, and for the single record and linear-elastic model adopted, the study examines whether the soil class changes which configuration produces the largest response compared with the fixed-base case. Whether such changes hold for other records and for nonlinear behavior remains to be confirmed.

2. Methodology

The structural models were developed and analyzed using SAP2000 Version 21. The RC beams and columns were modeled as three-dimensional frame elements, and rigid diaphragm constraints were assigned to the floor slabs to represent uniform movement within each floor. The masonry infill walls were represented using equivalent diagonal compression struts. The width of each strut was calculated based on the contact between the infill wall and the surrounding frame, as explained in Section 2.3.

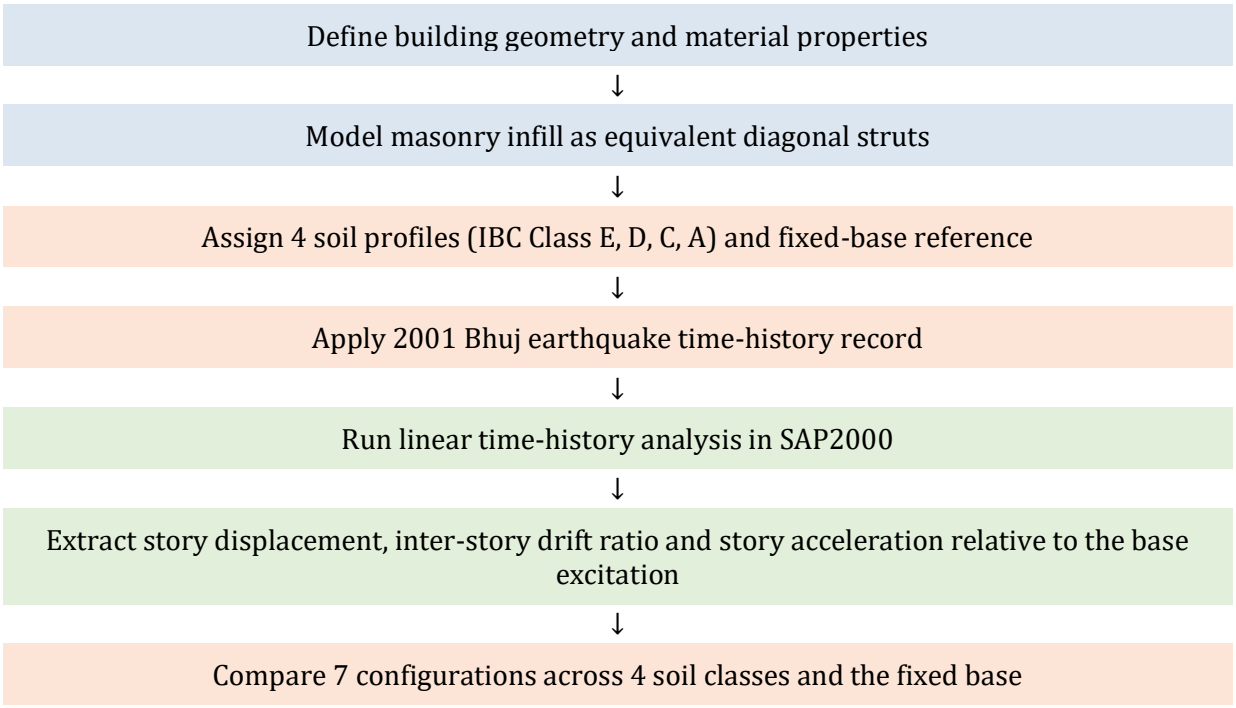

Fig. 1. Modeling and analysis workflow overview

The foundations were modeled as isolated pad footings placed 2 m below the ground surface. To study the effect of soil–structure interaction (SSI), four soil conditions were considered: soft soil, stiff soil, soft rock, and hard rock. All seven structural configurations were analyzed first with fixed supports and then with the four different soil conditions. This allowed the seismic response of the frames to be compared under fixed-base and SSI conditions.

2.1 Building Configuration and Material Properties

A 10-story, one-bay RC frame (5 m × 5 m plan, 3.5 m story height) with 230 mm × 600 mm beams and columns, a 150 mm slab, 230 mm infill walls, and 2000 mm × 2000 mm × 500 mm isolated (pad) footings at 2 m depth (Fig. 6) was used; material properties are listed in Table II. In the soft-story configurations the ground story was left without infill (open ground story), while all upper stories were infilled (Fig. 4).

Table 2. Mechanical properties of structural materials

Material	Strength	Elastic Modulus (MPa)	Unit Weight (kN/m^3)	Poisson's Ratio
Concrete	fck = 25 MPa	25,000	25	0.20
Masonry infill	5 MPa	2,750	20	0.18
Steel reinforcement	fy = 415 MPa	1.99×10^5	78.5	0.30

2.2 Soil Classification

Four soil types were modeled beneath the isolated footings, representing IBC 2006 [35] site classes E, D, C and A. The soil domain measured 100 m × 100 m in plan and 30 m in depth in each case (boundary conditions are described in Section 2.5); soil properties are listed in Table III. The fundamental period of each 30 m soil column, estimated as $T_s = 4H/V_s$ [36], is listed in Table IV together with the predominant period of the input record (T_g = 0.27 s, Section 2.4). The soft-rock column (T_s = 0.24 s) is closest to the record, while the stiff- and soft-soil columns have periods 1.7 and 2.5 times longer.

Table 3. Engineering properties of soil media

Soil Type	IBC Class	Vs (m/s)	Unit Wt. (kN/m^3)	Elastic Mod. (kN/m^2)	μ
Soft soil	E	175	15	1.2175×10^5	0.30
Stiff soil	D	258	17	3.0×10^5	0.30
Soft rock	C	507	22	1.5×10^6	0.30
Hard rock	A	2500	24	3.7×10^7	0.30

Table 4. Fundamental period of the 30 m soil columns (H = 30 m) relative to the predominant period of the Bhuj record (T_g = 0.274 s)

Soil type	IBC class	Vs (m/s)	Ts = 4H/Vs (s)	Ts/Tg
Soft soil	E	175	0.69	2.51
Stiff soil	D	258	0.47	1.70
Soft rock	C	507	0.24	0.86
Hard rock	A	2500	0.05	0.18

2.3 Equivalent Diagonal Strut Modeling of Masonry Infill

The stiffness contribution of a masonry infill panel restrained within an RC frame is represented by an equivalent diagonal compression strut of the same thickness as the infill wall, following the classical formulation of Hendry [37] in the form given by Agarwal and Shrikhande [38] (Fig. 3). The effective strut width, w, is obtained from

$$w = 0.5\sqrt{\alpha h^2 + \alpha L^2} \tag{1}$$

where α_h and α_L are the contact lengths between the panel and the column and between the panel and the beam, respectively [37, 38]:

$$\alpha_h = \frac{\pi}{2}\left(\frac{E_f I_c h}{2E_m t \sin 2\theta}\right)^{1/4} \tag{2}$$

$$\alpha_L = \pi\left(\frac{E_f I_b h}{E_m t \sin 2\theta}\right)^{1/4} \tag{3}$$

in which $E_f = 5000\sqrt{f_{ck}} = 25 \times 10^6$ kN/m^2 and $E_m = 550\, f_m = 2.75 \times 10^6$ kN/m^2 (f_m = 5 MPa [39]) are the elastic moduli of the frame concrete and the masonry, $I_c = 4.14 \times 10^{-3}$ m^4 is the second moment

of area of the 230 mm × 600 mm column, $I_b = 1.7465 \times 10^{-3}$ m⁴ that of the beam web below the slab (230 mm × 450 mm), h = 3.0 m the clear height of the panel, t = 0.23 m the infill thickness and $\theta = \tan^{-1}(h/L)$ the inclination of the strut, with clear panel lengths L = 4.4 m in the x direction and 4.77 m in the y direction ($\theta_x = 34.3°$, $\theta_y = 32.2°$). These values give $\alpha_h = 1.125$ m, $\alpha_L = 2.160$ m and $w_x = 1.218$ m in the x direction, and $\alpha_h = 1.135$ m, $\alpha_L = 2.223$ m and $w_y = 1.248$ m in the y direction.

Each panel was represented by two diagonals (Figs. 3 and 4) so that the infill resists lateral load in both directions. Because a linear analysis cannot deactivate a strut when it goes into tension, each diagonal was assigned half of the strut area (w·t/2), so that the two diagonals together provide the lateral stiffness of one compression strut in either loading direction. The struts were pin-connected at the beam–column joints and carry axial force only.

For panels with openings, the strut width was derived from the lateral stiffness of a finite element (shell) model of the perforated panel. A lateral load of 10 kN was applied in the plane of the panel, and the resulting displacement gave a stiffness K = 2.015 × 10⁵ kN/m for the solid panel, 1.0 × 10⁵ kN/m for the panel with two 1.2 m × 1.5 m windows (30% opening) and 0.5 × 10⁵ kN/m for the panel with a central opening (50%). The equivalent strut width of a perforated panel was then obtained from its stiffness K_{op} as

$$w_{op} = \frac{K_{op}\, L}{E_m\, t} \tag{4}$$

which gives the widths listed in Table V. The corresponding reduction factors $R = w_{op}/w$ are 0.571 and 0.286 in the x direction for 30% and 50% openings. For comparison, the empirical relation of Al-Chaar [40] gives 0.574 and 0.350, and that of Asteris et al. [41] about 0.21 and 0.08, so the adopted reduction lies within the published range and almost coincides with Al-Chaar's value for 30% openings.

Table 5. Lateral stiffness of the infill panels and equivalent strut widths

Opening	Panel stiffness K (kN/m)	w_x (m)	w_y (m)	$R = w_{op}/w$ (x / y)
0% (solid)	2.015 × 10⁵	1.218	1.248	1.000 / 1.000
30% (two 1.2 m × 1.5 m windows)	1.0 × 10⁵	0.696	0.754	0.571 / 0.604
50% (central opening)	0.5 × 10⁵	0.348	0.377	0.286 / 0.302

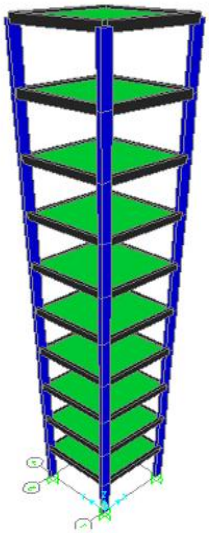

Fig. 2. Finite element model of the bare frame

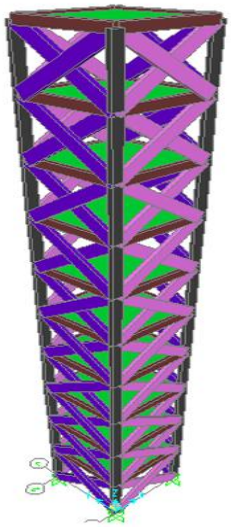

Fig. 3. Finite element model of the infill wall

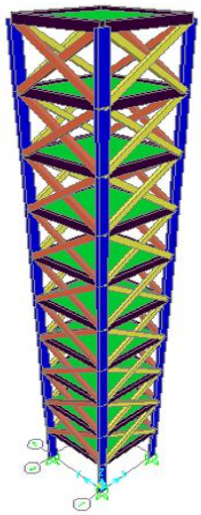

Fig. 4. Finite element model of the infill wall with a soft story

2.4 Ground Motion

The 2001 Bhuj earthquake accelerogram (Fig. 5) was used as the input ground motion: local magnitude 7.6, predominant frequency 3.65 Hz (T_g = 0.274 s) and duration 133.5 s. The record was scaled to a peak ground acceleration (PGA) of 0.1 g. In SAP2000, a time-history acceleration load acts as a uniform support excitation at all restrained joints.

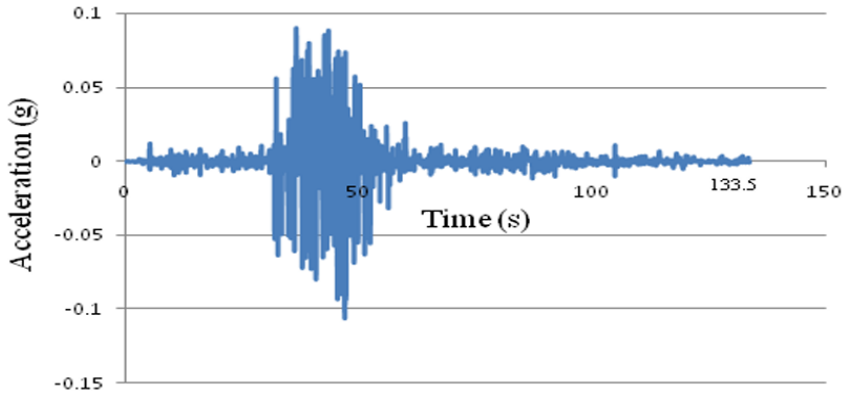

Fig. 5. Input earthquake acceleration time-history used for the dynamic analysis (2001 Bhuj earthquake in Gujarat, India)

The record was therefore applied at the base of the 30 m soil block (and at its restrained lateral boundary nodes), not at the ground surface, so the motion reaching the footings includes the amplification of each soil column. For the fixed-base models, the same record was applied directly at the column bases.

2.5 Finite Element Modeling in SAP2000

All models were developed in SAP2000. Beams and columns were modeled as linear-elastic frame elements, slabs as rigid diaphragms and masonry infill as equivalent diagonal struts. The mass was derived from the self-weight of the members, a superimposed dead load of 1.5 kN/m^2, an infill line load of 14 kN/m (3.0 m × 0.23 m × 20 kN/m^3) and a live load of 2.5 kN/m^2, and was lumped at the joints of every floor. The soil was modeled as a three-dimensional linear-elastic continuum of solid elements bonded to the isolated footings, giving direct (coupled) soil–structure interaction (Fig. 6). The bottom and lateral boundary nodes of the soil block were restrained, as shown in Fig. 6, and no viscous (Lysmer–Kuhlemeyer [42]) dampers or infinite elements were used. The plan extent of 100 m (50 times the footing width and about three times the building height) was chosen to approach free-field conditions and to limit the influence of waves reflected from the lateral boundaries on the footing response. Without absorbing boundaries, however, some wave trapping in the bounded soil block cannot be excluded; its possible effect on the peak accelerations is discussed in Section 3.6. Linear time-history analysis was performed with 5% damping. The outputs are the peak story displacement relative to the base of the model, the peak story acceleration, the floor response spectra (computed from the story acceleration histories) and the inter-story drift ratio (Section 3.5). The story accelerations are the SAP2000 joint accelerations relative to the base excitation; they therefore exclude the input ground acceleration and can be smaller than the input PGA at stiff lower stories. The acceleration amplification factor is defined as

$$AF = \frac{a_{roof,max}}{PGA} \tag{5}$$

where $a_{roof,max}$ is the peak roof acceleration relative to the base of the model and PGA = 0.1 g is the peak acceleration of the scaled input record.

3. Results and Discussion

Table VI(A) presents the predominant response period obtained from the 5% damped floor response spectra. Since modal periods were not extracted, this period is used to describe the dynamic response of the soil–structure system. For fixed-base models, the periods range from 0.78

s for the 50% opening frame to 1.2 s for the bare frame. Soft-story frames generally have longer periods (0.86–1.08 s) than regular frames (0.78–0.86 s). They also show the highest roof displacement, about 73 mm, compared with 60–70 mm for regular frames. The soft-story and bare frames reach a roof acceleration of about 0.475 g (AF = 4.75).

Thus, under fixed-base conditions, the soft-story frame gives the highest overall response. However, the results in Sections 3.1–3.4 show that the critical configuration changes when soil–structure interaction is considered.

Table 6(A). Predominant period (s) of the response for the fixed base and each soil class

Configuration	Fixed base	Soft soil (E)	Stiff soil (D)	Soft rock (C)	Hard rock (A)
Bare frame	1.20	0.42	0.30	1.42	0.25
Full infill	0.86	1.90	0.30	0.26	1.40
Full infill + soft story	1.08	0.52	0.52	0.52	1.60
30% opening	0.80	0.50	0.30	0.20	1.38
30% opening + soft story	0.90	0.52	0.52	0.16	0.50
50% opening	0.78	0.52	0.30	0.30	1.40
50% opening + soft story	0.86	0.52	0.30	0.50	0.50

Table 6(B). Base Shear of the response for the fixed base and each soil class

Configuration	Fixed base (kN)	Soft soil E (kN)	Stiff soil D (kN)	Soft rock C (kN)	Hard rock A (kN)
Bare frame	850	700	1,050	900	800
Full infill	1,250	950	1,450	1,300	1,150
Full infill + soft story	1,100	800	1,250	1,050	950
30% opening	1,150	900	1,350	1,200	1,050
30% opening + soft story	1,000	750	1,150	1,000	900
50% opening	1,050	850	1,250	1,100	1,000
50% opening + soft story	950	700	1,100	950	850

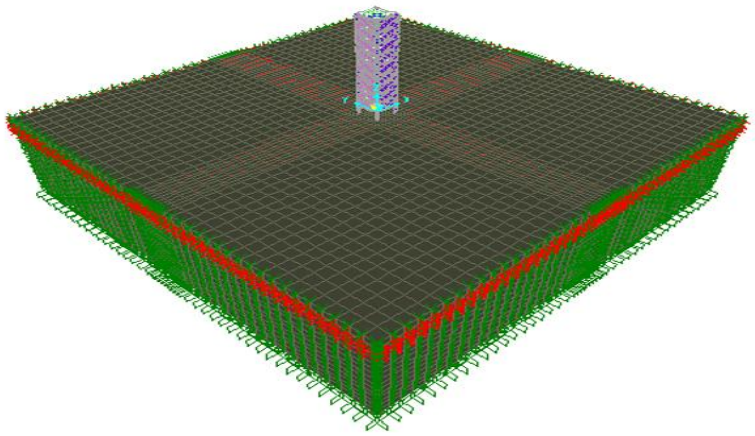

Fig. 6. Geometry and boundary conditions of the soil–structure model

The base shear results show that full infill buildings have higher base shear compared with bare frames because the infill increases the overall stiffness and seismic resistance of the structure. As the percentage of openings increases from 30% to 50%, the base shear generally decreases due to reduced infill stiffness. The introduction of a soft story also reduces the base shear compared with the corresponding infilled models. Among the soil conditions, Stiff Soil D generally gives higher base shear, while Soft Soil E gives lower values. Overall, the results show that infill configuration and soil–structure interaction significantly affect the seismic response of the building.

3.1 Effect of Soft Soil (Class E, Vs = 175 m/s)

Under soft soil conditions, displacement was similar for most configurations, except for the fully infilled frame without a soft story, which exhibited the highest roof displacement (241 mm). The bare frame showed the lowest roof displacement (83 mm), while the remaining configurations followed comparable displacement profiles (Fig. 7). These results indicate that soft-story irregularity and wall openings have only a minor influence on roof displacement in soft soil, whereas the fully infilled frame without a soft story shows the largest roof displacement. Its nearly linear displacement profile and its long predominant response period (1.9 s, Table VI(A)) indicate that this response is dominated by rocking of the stiff infilled frame on the soft soil. In the soft-story frames, by contrast, deformation concentrates in the open ground story (about 63 mm at the first floor), which governs their drift (Section 3.5). The corresponding acceleration profiles are presented in Fig. 8.

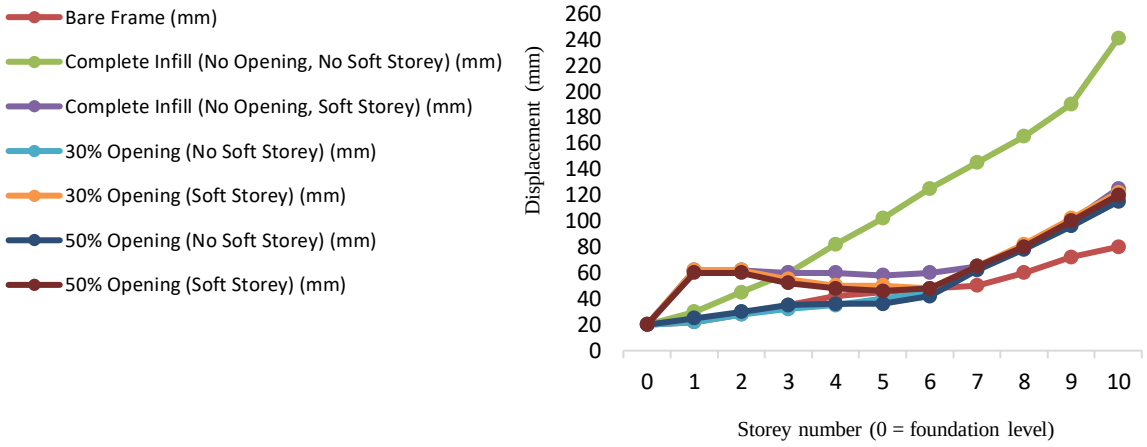

Fig. 7. Story displacement under soft soil conditions

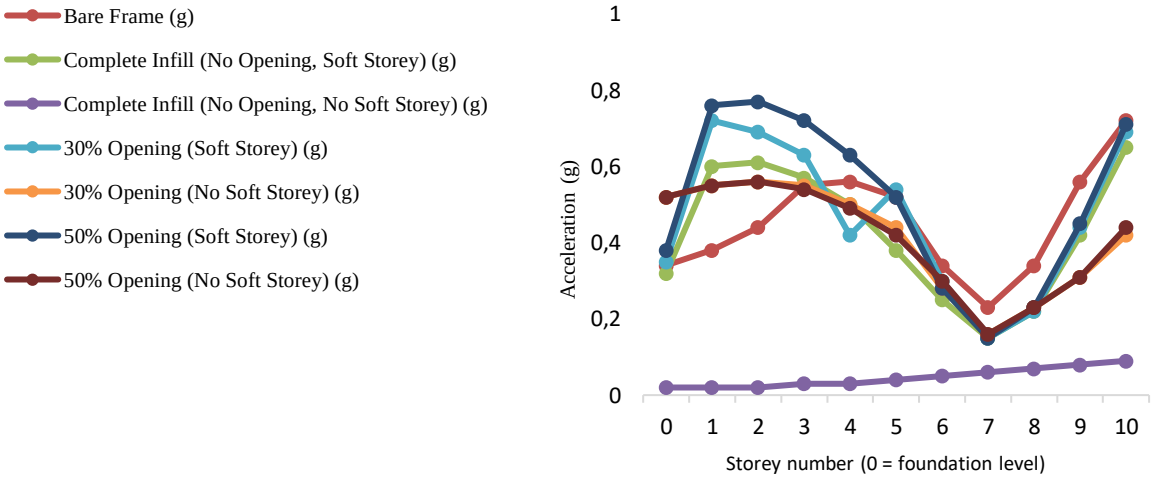

Fig. 8. Story acceleration under soft soil conditions

From the analysis shown in Fig. 8, it is found that in the infill frames with a soft story and the bare frame, the acceleration is amplified up to 7.4 times at the top of the building, with a peak acceleration of 0.74g for soft soil, whereas the fully infilled frame without a soft story is amplified 0.96 times, with a peak acceleration of 0.096g. The low acceleration of this frame, together with its large displacement, is consistent with a long-period rocking response.

3.2 Effect of Stiff Soil (Class D, Vs = 258 m/s)

Under stiff soil conditions (Fig. 9), the bare frame exhibits the lowest roof displacement (65 mm), while the fully infilled frame and the 30% and 50% opening frames without a soft story show the

highest values (≈120 mm). Soft-story frames have smaller roof displacements (≈108 mm) and, as the drift ratios in Section 3.5 confirm, smaller maximum inter-story drifts (0.43–0.54% against 0.86–0.91% for the frames without a soft story), and thus a lower drift demand on stiff soil. The effect of infill openings on displacement is minimal, with response profiles remaining close to those of the fully infilled frame. The corresponding acceleration responses are presented in Fig. 10.

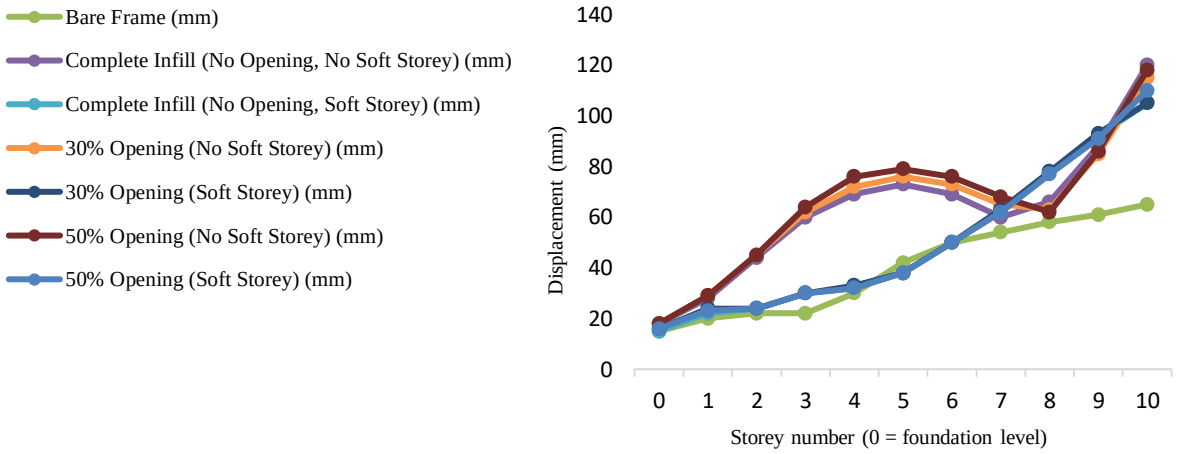

Fig. 9. Story displacement under stiff soil conditions

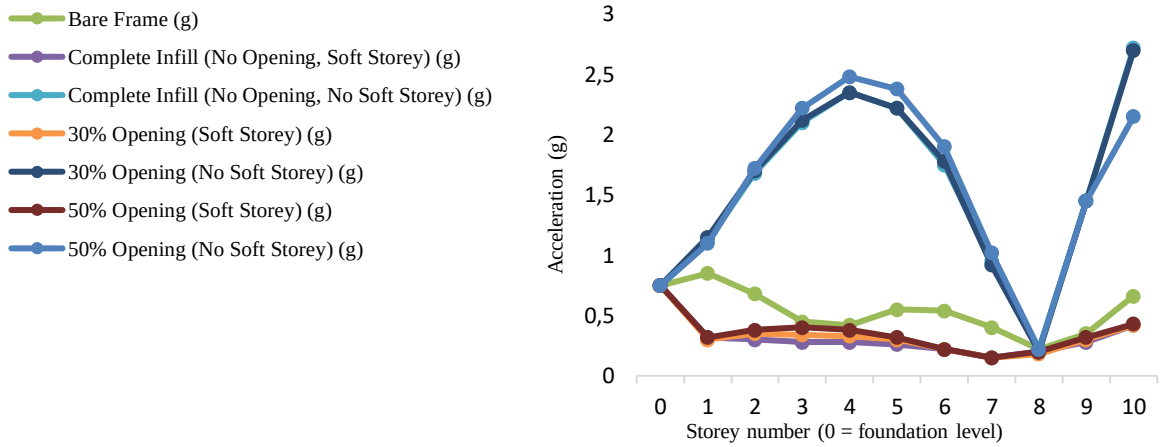

Fig. 10. Story acceleration under stiff soil conditions

From Fig. 10, the infill frames with a soft story and the bare frame show acceleration amplified up to 6.76 times at the top of the building, reaching a peak of 0.67g under stiff soil. In contrast, the infill frames without a soft story show much greater amplification, up to 27 times, with a peak acceleration of 2.7g at the roof. The floor response spectra of these frames peak at 0.3 s (Table VI(A)), close to the predominant period of the input record (0.274 s); this resonance is discussed in Section 3.6.

3.3 Effect of Soft Rock (Class C, Vs = 507 m/s)

From the analysis in Fig. 11, under soil-structure interaction with soft rock, the bare frame shows a top displacement of 92 mm, while the fully infilled frame with a soft story records the maximum, at 97 mm. Soft-story frames with 50% and 30% openings displace 88 mm and 82 mm respectively, while infill frames without a soft story range from 66 mm to 70 mm. This confirms that soft-story infilled frames are more vulnerable to earthquake damage, while openings have little effect on frames without a soft story. Fig. 12 shows the floor-wise acceleration profiles for the bare frame and all infill configurations, both with and without a soft story and openings.

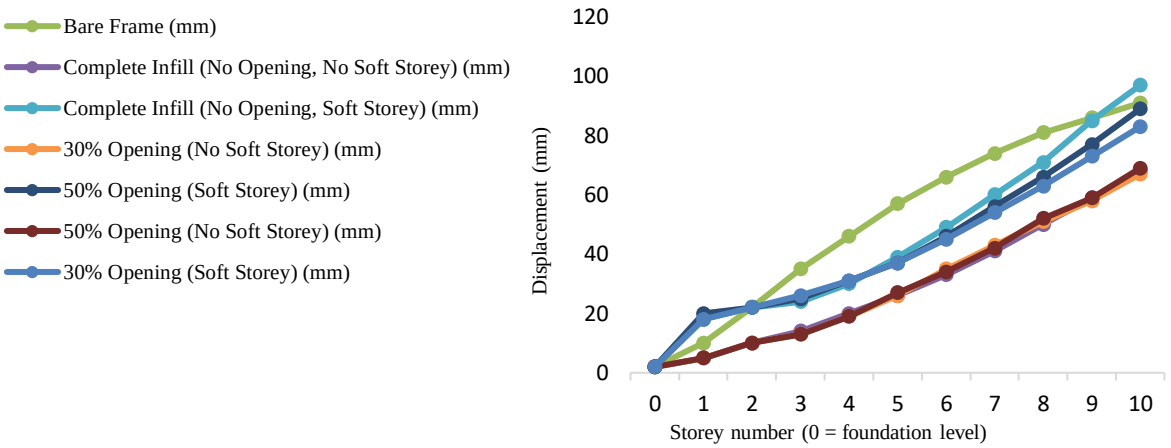

Fig. 11. Story displacement under soft rock conditions

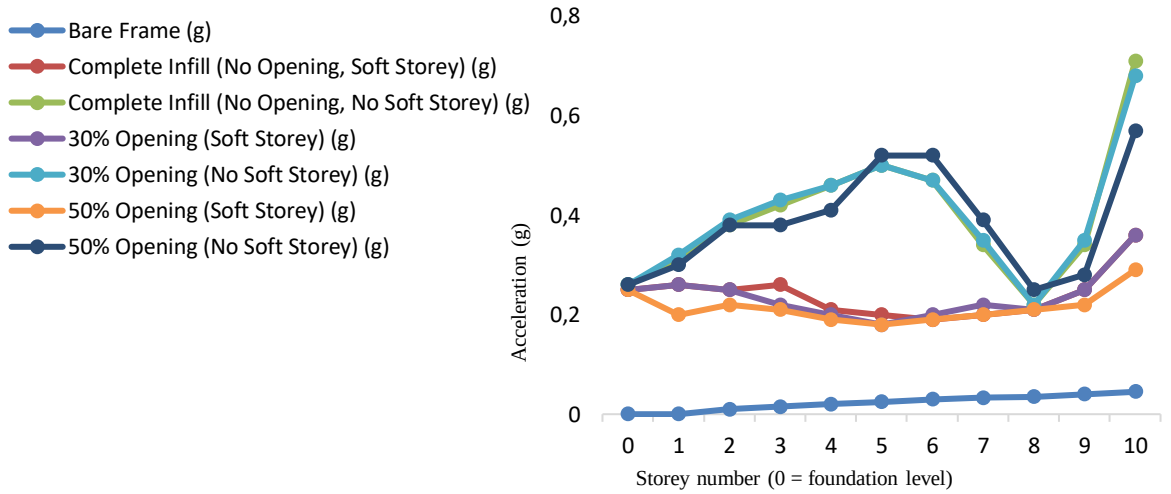

Fig. 12. Story acceleration under soft rock conditions

From Fig. 12, the infill frame with a soft story shows acceleration amplified up to 3.52 times at the top of the building, reaching a peak of 0.352g under soft rock conditions. The fully infilled frame without a soft story shows greater amplification, at 7.12 times with a peak of 0.712g, while the bare frame amplifies only 0.46 times, peaking at 0.046g. The response spectrum of the fully infilled frame without a soft story peak at 0.26 s, again close to the predominant period of the record, whereas that of the bare frame peaks at 1.42 s, far from it. The bare-frame value is below the input PGA because the reported accelerations are relative to the base excitation (Section 2.5).

3.4 Effect of Hard Rock (Class A, Vs = 2500 m/s)

Fig. 13 shows that, under soil-structure interaction with hard rock, the bare frame has the minimum top displacement, at 62 mm, while the fully infilled frame without a soft story records the maximum, at 100 mm. Frames without a soft story with 30% and 50% openings both show 86 mm, while soft-story frames with full infill, 30%, and 50% openings displace 85 mm, 75 mm, and 70 mm respectively. This shows that infilled frames without a soft story have the largest roof displacements on hard rock, although the soft-story frames still show the largest ground-story drift (Section 3.5), while openings have little effect in that configuration. Fig. 14 shows the floor-wise acceleration profiles for the bare frame and all infill configurations, with and without a soft story and openings. From Fig. 14, the infill frames with a soft story and 30% or 50% openings show acceleration amplified up to 2.63 times at the top of the building, reaching a peak of 0.263g under hard rock, whereas the fully infilled frame with a soft story reaches 0.065g. The frames without a soft story show a much lower peak acceleration of 0.045g, while the bare frame peaks at 0.236g. The frames without a soft story respond at predominant periods of about 1.4 s (Table VI(A)), far from the dominant period of the record.

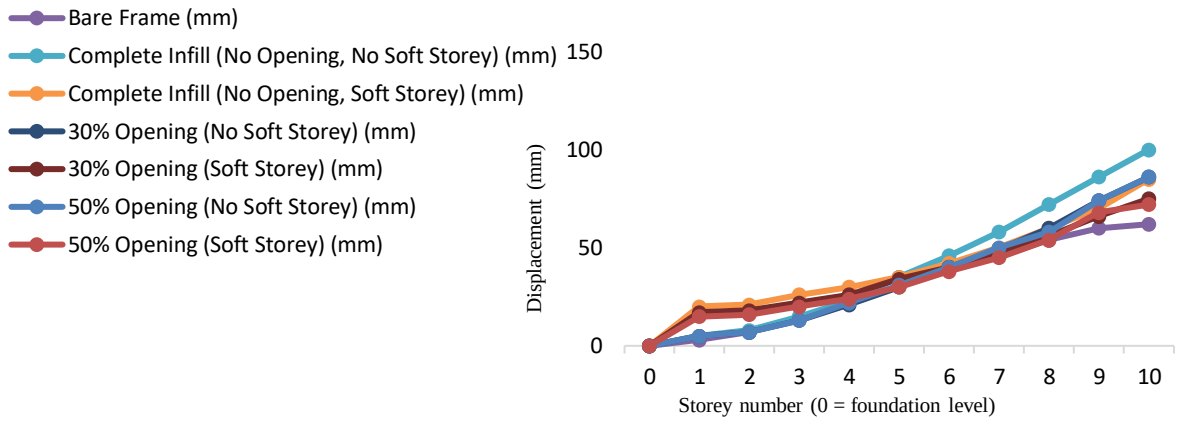

Fig. 13. Story displacement under hard rock conditions

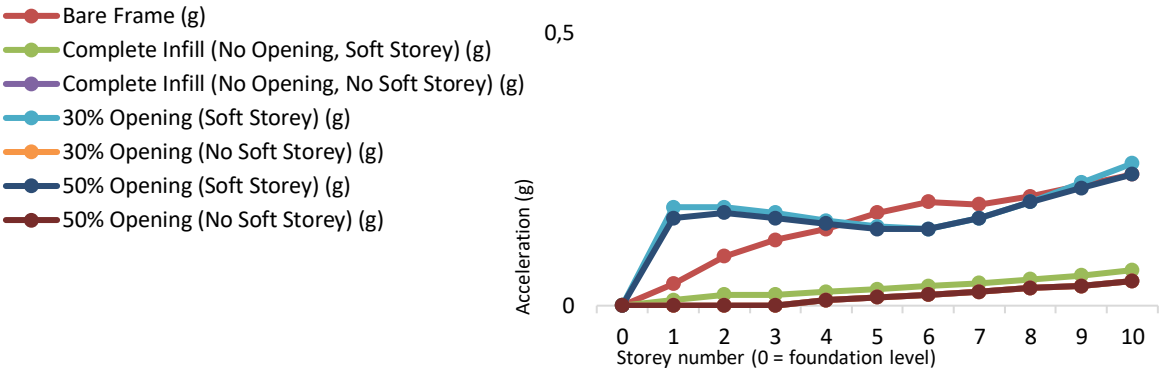

Fig. 14. Story acceleration under hard rock conditions

3.5 Inter-Story Drift Ratio

Because roof displacement does not reveal where deformation concentrates, the inter-story drift ratio of story i was evaluated as

$$IDR_i = \frac{u_i - u_{i-1}}{h_i} \times 100 \quad (6)$$

where u_i is the peak displacement of floor i and h_i = 3.5 m is the story height. The IDR profiles are shown in Fig. 15 and the maximum values in Table VII. Because only peak-displacement envelopes are available, and peak floor displacements need not occur at the same instant, these drift ratios are approximate; they are used to compare configurations and soil classes.

On soft soil, soft rock and hard rock, the largest drift occurs in the ground story of a soft-story frame: 1.14–1.20% on soft soil, 0.46–0.51% on soft rock and 0.43–0.57% on hard rock. These values are three to six times the ground-story drift of the corresponding frames without a soft story (0.09–0.29%), whose maximum drift occurs in the upper stories. On these soils the soft-story frames are therefore the most critical configuration for drift-controlled damage, even where their roof displacement is smaller, and the ground-story drift of the soft-story frames on soft soil is 2.1–2.7 times the hard-rock value, showing that soil flexibility amplifies the soft-story mechanism rather than relieving it. Stiff soil is the exception. There, the frames without a soft story, which respond in resonance with the input (Section 3.6), reach the largest drifts of that soil (0.86–0.91%, in the top story), whereas the soft-story frames reach 0.43–0.54% in the upper stories and only 0.20–0.23% in the ground story. The governing configuration for drift therefore also depends on the soil class. For the fully infilled frame on soft soil, part of the 0.71% upper-story drift comes from rigid-body rotation (rocking) of the building and does not deform the story. For reference, IS 1893 (Part 1) [43] limits story drift to 0.4% under design forces. The ground-story drift of the soft-story frames

on soft soil exceeds this value by a factor of three, although the input PGA of 0.1 g is well below the design level for high-seismicity zones.

Table 8. Maximum inter-story drift ratio (%)

Configuration	Soft soil (E)	Stiff soil (D)	Soft rock (C)	Hard rock (A)
Bare frame	0.34	0.34	0.37	0.34
Full infill	0.71	0.91	0.26	0.40
Full infill + soft story	1.20	0.43	0.46	0.57
30% opening	0.57	0.86	0.26	0.40
30% opening + soft story	1.20	0.43	0.46	0.49
50% opening	0.57	0.91	0.29	0.46
50% opening + soft story	1.14	0.54	0.51	0.43

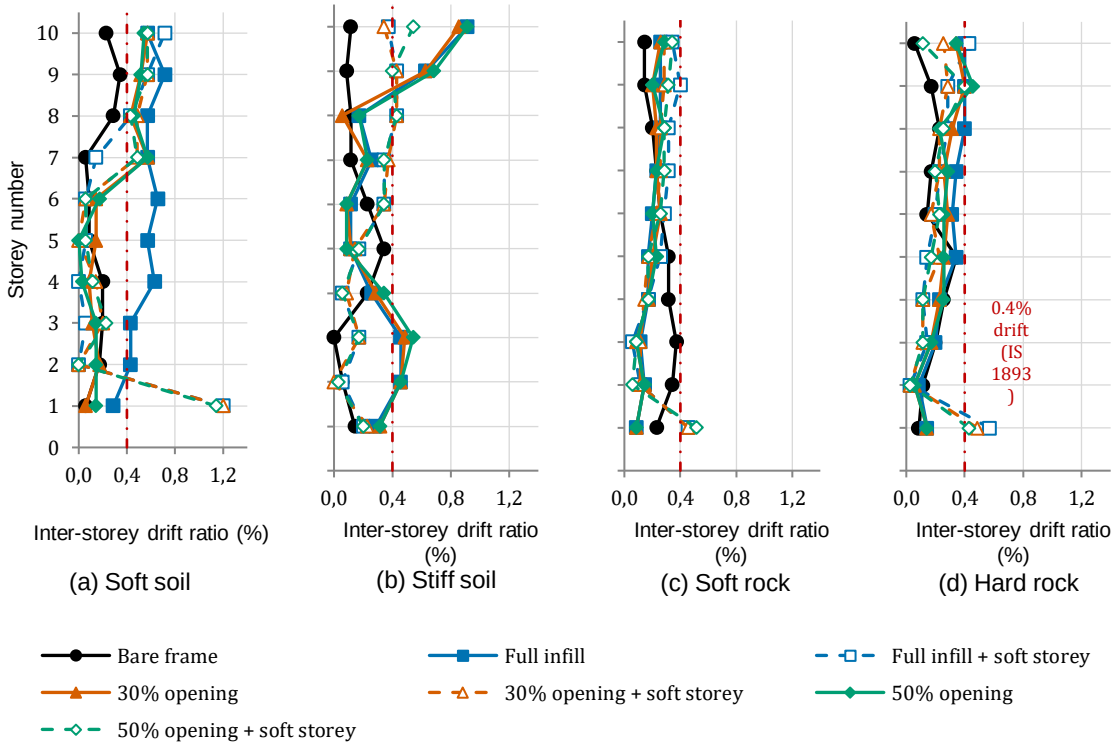

Fig. 15. Inter-story drift ratio profiles: (a) soft soil, (b) stiff soil, (c) soft rock, (d) hard rock. The dash-dot line marks the 0.4% drift limit of IS 1893 (Part 1) [43]

3.6 Physical Interpretation of the Acceleration Amplification

Four mechanisms are considered for the very high accelerations of the infilled frames without a soft story on stiff soil (up to 2.7 g, AF ≈ 27). Resonance. The input record has a predominant frequency of 3.65 Hz (Tg = 0.274 s). The floor response spectra of the three infilled frames without a soft story on stiff soil all peak at 0.3 s (Table VI(A)), with roof spectral accelerations of 20–21 g. Their response is therefore concentrated at the dominant period of the input, which is the condition for resonance. The same frames on soft rock respond at 0.20–0.30 s and show the second-highest amplification (AF up to 7.1). On soft soil and hard rock, their predominant periods (0.5–1.9 s and about 1.4 s) are far from Tg, and their roof accelerations are low (AF ≤ 4.4 and about 0.45). The soft-story frames on stiff soil respond at 0.52 s, away from the energy of the input, and reach much smaller accelerations. The stiff-soil column itself (Ts = 0.47 s, Table IV) lies between the record period and these structural periods and may further amplify the motion reaching the footings. The extreme amplification is therefore attributed to resonance between the soil–structure system and the dominant frequency of the input motion.

Higher-mode response. The sharp minimum of peak acceleration at stories 7–8 followed by a rise at the roof (Figs. 8, 10 and 12) is characteristic of a strong second-mode contribution. For a flexural (braced-cantilever) response, which is typical of fully infilled frames, the node of the second mode lies at about 0.78 of the height, i.e. between stories 7 and 8 of this building [32]. The story masses are assigned at every floor through the slab, beam, column and infill loads (Section 2.5), so the dip is not caused by a floor without mass. The same story-8 minimum also appears in the displacement profiles of the frames without a soft story on stiff soil (Section 3.2).

Bounded soil domain. The lateral and bottom boundaries of the soil block are restrained and have no absorbing elements (Section 2.5). Waves radiated by the footing can therefore be partly reflected back, reducing the radiation damping that a semi-infinite soil would provide and possibly trapping energy in the soil column. This may contribute to the peak accelerations on the softer soils, and the values should be regarded as upper estimates.

Linear-elastic behavior. A floor acceleration of 2.7 g would require an inertial force far above the lateral strength of a real infilled frame. In an actual earthquake, diagonal cracking of the infill at small drifts, sliding along bed joints, and cracking and yielding of the concrete would reduce the stiffness, lengthen the period and dissipate energy, capping the floor accelerations well below this value. The linear-elastic accelerations reported here therefore indicate the elastic demand and the relative sensitivity of each configuration to the soil class, not the accelerations that would actually be attained. This is listed as a limitation in Section 5.

4. Comparative Analysis of Results

Table 8 compares the present results quantitatively with published studies of masonry-infilled RC frames with openings, soft stories or SSI.

Table 8. Quantitative comparison with related studies

Study	Configuration and input	Displacement / period	Drift	Other findings
Messaoudi et al. [26]	6-story, 3-bay; fixed base; strut model	Full infill: top displacement −54% vs bare frame	Soft-story layouts: drift up to +264% vs full infill	Base shear +278% (full infill vs bare)
Furtado et al. [1]	4-story; fixed base; nonlinear dynamic	Openings: natural frequency ≈ −20%	–	Openings: initial stiffness and peak base shear ≈ −20%
Amritha and Prasanth [25]	6- and 11-story; direct 3D soil; nonlinear time-history, 0.36 g	Roof displacement, soft vs stiff sand: +3.6% to +20.7%	IDR 0.73–1.4% with SSI vs 0.35–0.36% fixed base	Fixed base underestimated damage states
Santa-Ana-Lozada et al. [15]	Irregular 10-story; 3D nonlinear soil; 42 records	Period elongation 31% and 75%	First-story drift up to 5× fixed base	Damage index > 1 despite meeting drift limits
Karki et al. [31]	Infilled frame; NNBC soil types; static and pushover	Period and peak displacement increase as soil rigidity decreases	IDR increases with flexible base	Fixed base gave higher capacity and damage level
Present study	10-story, one-bay; direct 3D elastic soil; linear time-history, Bhuj scaled to 0.1 g	Roof displacement, soft soil vs hard rock: 241 vs 100 mm (full infill); predominant period 0.86 s (fixed base) to 1.9 s (soft soil) for full infill	Soft-story ground story: 1.14–1.20% (soft soil), 0.43–0.57% (hard rock), 3–6× regular frames; on stiff soil the regular frames govern (0.86–0.91%)	Roof AF up to ≈ 27 (elastic) for regular infilled frames on stiff soil, responding at the record period

Amritha and Prasanth [25] reported inter-story drift ratios of 0.73–1.4% with SSI, against about 0.35% for the fixed base, and roof displacement increases of up to about 21% between stiff and soft sand. The present ground-story drift of 1.14–1.20% for the soft-story frames on soft soil is of the same order, although it results from a record scaled to a PGA of only 0.1 g compared with their 0.36 g. The soil effect on roof displacement is much larger here (up to 2.4 times between hard rock and soft soil for the fully infilled frame). This is because the slender one-bay frame (height-to-width ratio 7) on pad footings rocks strongly on soft soil, whereas their 3 × 3-bay buildings rested on a raft. Santa-Ana-Lozada et al. [15] found that SSI increased the first-story drift of an irregular ten-story infilled building on soft soil up to five-fold and lengthened the fundamental period by 31–75%. The present results agree on the concentration of drift in the lowest story: on soft soil, the ground-story drift of the soft-story frames is 2.1–2.7 times the hard-rock value. For the fully infilled frame, the predominant response period on soft soil (1.9 s) is more than twice the fixed-base value (0.86 s), a larger shift than their 31–75% because rocking of the slender one-bay frame dominates its response on soft soil.

For fixed-base frames, Messaoudi et al. [26] reported drift increases of up to 264% when infill was omitted from individual stories. This is consistent with the three- to six-fold ratio found here between the ground-story drift of soft-story and regular frames on soft soil, soft rock and hard rock. Furtado et al. [1] found that openings reduced stiffness and base shear by about 20%; in the present model, 30–50% openings reduced the roof displacement of the soft-story frames by up to 18% on hard rock and had little effect on the regular frames. Karki et al. [31], using static procedures, likewise found that the period, peak floor displacement and inter-story drift increased as soil rigidity decreased. The present results reproduce this trend for the drift of the soft-story frames and for the roof displacement of the regular frames, but not for every response quantity: floor accelerations of the regular infilled frames peaked on stiff soil rather than soft soil, an effect that static procedures cannot capture.

5. Conclusions

This paper presented a parametric study of the seismic response of a ten-story masonry-infilled RC frame with 0%, 30% and 50% infill openings, with and without a ground soft story, on four soil classes and a fixed base, using linear time-history analysis with direct soil–structure interaction. The main conclusions and their implications for design are as follows.

- The soil class changes which configuration governs each response parameter. On soft soil, the fully infilled frame without a soft story governed roof displacement, largely through rocking. On stiff soil, the regular infilled frames governed floor acceleration. The soft-story frames governed inter-story drift on soft soil, soft rock and hard rock, whereas on stiff soil the regular infilled frames, which responded in resonance with the input, governed both drift and floor acceleration. A ranking based on a single response parameter, or on a fixed-base analysis, can therefore misidentify the critical configuration.
- Roof displacement is not an adequate measure of risk for soft-story frames. On hard rock their roof displacement was smaller than that of the regular frames, yet their ground-story drift was three to six times larger (as it was on soft soil and soft rock) and was further amplified by soil flexibility (2.1–2.7 times from hard rock to soft soil). Drift checks for open-ground-story buildings on soft sites should therefore be made with a flexible-base model, in addition to the soft-story strengthening required by IS 1893 (Part 1) [43].
- The effect of SSI on floor acceleration depends on how the soil–structure system responds relative to the dominant period of the ground motion. On a fixed base, the soft-story frames were the critical configuration; on stiff soil, the regular infilled frames responded at the predominant period of the record and produced the largest elastic floor accelerations of the study. Fixed-base design spectra, and code provisions that permit reduced base shear for SSI, may therefore be unconservative for stiff infilled buildings on stiff soil sites, particularly for acceleration-sensitive non-structural components.
- As a screening criterion, an SSI analysis may be considered in place of the fixed-base assumption when the structure-to-soil stiffness ratio $h/(V_sT)$ exceeds about 0.1 [34], where h is the effective height of the building and T its fixed-base period, or when the flexible-base

period lies within about ±30% of the site period $T_s = 4H/V_s$. The second criterion is suggested by the present results and should be verified with further records. In these cases, the design spectrum should be entered at the flexible-base period, and both drift and floor acceleration should be checked against the governing soil class rather than a single assumed worst case.

- Openings of 30–50%, modeled by reducing the strut width according to the finite element stiffness of the perforated panel, reduced the roof displacement of the soft-story frames by up to 18% and had little effect on the regular frames. Their influence was secondary to that of the soft story and the soil class.

5.1 Limitations

The study has some limitations. First, only the 2001 Bhuj earthquake record, scaled to 0.1 g PGA, was used; therefore, the results may vary with different ground motions. Second, the frame, infill, and soil were assumed to behave linearly, and effects such as cracking, yielding, soil nonlinearity, uplift, and sliding were not considered. Hence, the reported acceleration amplification and drift values represent elastic responses. Third, the soil model used restrained boundaries without absorbing elements, which may affect the peak response. The study also considered a single one-bay frame, while out-of-plane infill behavior was neglected. In addition, predominant response periods were used instead of modal periods. Future studies should consider nonlinear analysis with multiple earthquake records, absorbing boundaries, multi-bay frames, layered soils, and groundwater effects to provide a more comprehensive assessment of soil–structure interaction.

Acknowledgement

The authors gratefully acknowledge S J C Institute of Technology and R R Institute of Technology for their support during this research.

References

[1] Furtado H, Rodrigues H, Arêde A. Effect of the openings on the seismic response of an infilled reinforced concrete structure. Buildings. 2022;12(11):2020. https://doi.org/10.3390/buildings12112020

[2] Kativale D, Kurlapkar R, Shendkar MR. A comprehensive review on the influence of masonry infill wall properties and opening configurations on the seismic response of RC buildings. E3S Web Conf. 2026;702:06007. https://doi.org/10.1051/e3sconf/202670206007

[3] Shendkar MR, Kontoni DPN, Işik E. Determination of the seismic vulnerability of infilled RC buildings according to the quadrants assessment method. Asian J Civ Eng. 2024;25:1-10. https://doi.org/10.1007/s42107-023-00904-x

[4] Haindl M, Burton H, Sattar S. Quantification of equivalent strut modeling uncertainty and its effects on the seismic performance of masonry infilled reinforced concrete frames. J Earthq Eng. 2024;28(1):41-61. https://doi.org/10.1080/13632469.2023.2171509

[5] Buch SH, Bhat JA, Bhat MD, Mirza MI. Seismic behavior of RC frames with choh-kat openings: a novel strut model approach. Bull Earthquake Eng. 2025;23(4):1639-1676. https://doi.org/10.1007/s10518-025-02112-1

[6] El-Kholy AM, Sayed SM, El-Assaly MM, Ismail MK. Modeling of masonry infilled RC frames with different aspect ratios using plastic hinge and equivalent strut. J Eng Appl Sci. 2025;72:18. https://doi.org/10.1186/s44147-024-00556-x

[7] Bhat ZM, Singh Y, Agarwal P. Cyclic testing and diagonal strut modelling of different types of masonry infills in reinforced concrete frames designed for modern codes. Eng Struct. 2024;317:118695. https://doi.org/10.1016/j.engstruct.2024.118695

[8] Londong Salu Y, Parung H, Tjaronge MW, Irmawaty R. Seismic performance of cellular lightweight concrete block panels as infilled wall in RC frames due to cyclic lateral loading. Eng Technol Appl Sci Res. 2024;14(5):16833-16839. https://doi.org/10.48084/etasr.8444

[9] Gu XL, Zhou T, Nagai K, Zhang H, Yu QQ. Prediction of seismic performance of a masonry-infilled RC frame based on DEM and ANNs. Eng Struct. 2024;316:118531. https://doi.org/10.1016/j.engstruct.2024.118531

[10] Milijaš A, Marinković M, Butenweg C, Klinkel S. Experimental investigation on the seismic performance of reinforced concrete frames with decoupled masonry infills: considering in-plane and out-of-plane load interaction. Bull Earthquake Eng. 2024;22:7489-7546. https://doi.org/10.1007/s10518-024-02012-w

[11] Chelapramkandy AK, et al. Influence of masonry infills on seismic performance of BRB-retrofitted low-ductile RC frames. Earthquake Eng Struct Dyn. 2025. https://doi.org/10.1002/eqe.4255

[12] Bapir LA, Wichtmann T, Prada-Sarmiento LF. Soil-structure interaction: a state-of-the-art review of modeling techniques and studies on seismic response of building structures. Front Built Environ. 2023;9:1120351. https://doi.org/10.3389/fbuil.2023.1120351
[13] Kadhim YM, Abdulridha AJ. Numerical simulation of soil-structure interaction on the seismic response of reinforced concrete buildings. Asian J Civ Eng. 2025;26:2869-2885. https://doi.org/10.1007/s42107-025-01349-0
[14] Requena-Garcia-Cruz MV, Bento R, Durand-Neyra P, Morales-Esteban A. Analysis of the soil structure-interaction effects on the seismic vulnerability of mid-rise RC buildings in Lisbon. Structures. 2022;38:599-617. https://doi.org/10.1016/j.istruc.2022.02.024
[15] Santa-Ana-Lozada P, Requena-Garcia-Cruz MV, Morales-Esteban A. Impact of the soil-structure interaction on the seismic vulnerability assessment of irregular masonry infilled RC buildings on soft soils. Bull Earthquake Eng. 2026. https://doi.org/10.1007/s10518-026-02549-y
[16] Attia A, Hadji T. Assessment of the soil structure inertial interaction effect on the behavior coefficient using simplified methods. Eng Technol Appl Sci Res. 2022;12(6):9420-9425. https://doi.org/10.48084/etasr.5266
[17] Wang J, Xie Y, Guo T. Predicting the influence of soil-structure interaction on seismic responses of reinforced concrete frame buildings using convolutional neural network. Buildings. 2023;13(2):564. https://doi.org/10.3390/buildings13020564
[18] Ebadi-Jamkhaneh M. Pounding risk assessment through soil-structure interaction analysis in adjacent high-rise RC structures. Buildings. 2024;14(9):2779. https://doi.org/10.3390/buildings14092779
[19] Wang J, et al. Seismic fragility assessment for existing RC frames considering structure-soil-structure interaction. Soil Dyn Earthquake Eng. 2025;192:109302. https://doi.org/10.1016/j.soildyn.2025.109302
[20] Forcellini D. Seismic fragility of tall buildings considering soil structure interaction (SSI) effects. Structures. 2022;45:999-1011. https://doi.org/10.1016/j.istruc.2022.09.070
[21] Firoj M, Bahuguna A, Kanth A, Agrahari R. Effect of nonlinear soil-structure interaction and lateral stiffness on seismic performance of mid-rise RC building. J Build Eng. 2022;59:105096. https://doi.org/10.1016/j.jobe.2022.105096
[22] Chakraborty A, Bhattacharya K, Sawant VA. Soil structure interaction effects on multistory asymmetric building subjected to earthquake loading. Indian Geotech J. 2024;55:303-314. https://doi.org/10.1007/s40098-024-00938-1
[23] Debbarma R, Verma Y. Effect of soil flexibility on seismic response of setback RC buildings considering raft foundation. Innov Infrastruct Solut. 2025;10(3):81. https://doi.org/10.1007/s41062-024-01820-y
[24] Camayang JPP, Padilla JA, De La Cruz AR, Bersamina JPL. Soil-structure interaction in seismic response and structural performance: a systematic review. Adv Struct Eng. 2026. https://doi.org/10.1177/13694332251353607
[25] Amritha N, Prasanth S. Seismic performances of reinforced concrete buildings with openings in unreinforced masonry infill walls: a soil-foundation-structure modelling approach. Front Built Environ. 2025;11:1667289. https://doi.org/10.3389/fbuil.2025.1667289
[26] Messaoudi A, Chebili R, Mohamed H, Rodrigues H. Influence of masonry infill wall position and openings in the seismic response of reinforced concrete frames. Appl Sci. 2022;12(19):9477. https://doi.org/10.3390/app12199477
[27] Dias-Oliveira J, Rodrigues H, Asteris PG, Varum H. On the seismic behavior of masonry infilled frame structures. Buildings. 2022;12(8):1146. https://doi.org/10.3390/buildings12081146
[28] Zhang X, Zhou Y, Liu X, Zheng Y, Qi Z. Study on seismic performance of RC frame structures considering the effect of infilled walls. Buildings. 2024;14(7):1907. https://doi.org/10.3390/buildings14071907
[29] Gamal YAS, Abdel Raheem SE, Oz I, Mansour MH. Masonry infill-bounding frame interaction impact on the seismic performance of MRF buildings. Structures. 2026;90:112455. https://doi.org/10.1016/j.istruc.2026.112455
[30] Manojlovski F, Tubaldi E, Sheshov V, et al. Flexible joints for seismic-resilient design of masonry-infilled RC frames. Sci Data. 2025;12:1266. https://doi.org/10.1038/s41597-025-05515-6
[31] Karki P, Pyakurel S, Utkarsh K. Seismic performance evaluation of masonry infill R.C. frame considering soil-structure interaction. Innov Infrastruct Solut. 2023;8(1):1-15. https://doi.org/10.1007/s41062-022-00979-6
[32] Chopra AK. Dynamics of structures: theory and applications to earthquake engineering. 5th ed. Hoboken, NJ: Pearson; 2017.
[33] Mylonakis G, Gazetas G. Seismic soil-structure interaction: beneficial or detrimental? J Earthq Eng. 2000;4(3):277-301. https://doi.org/10.1080/13632460009350372
[34] NIST. Soil-structure interaction for building structures, NIST GCR 12-917-21. Gaithersburg, MD: National Institute of Standards and Technology; 2012.
[35] International Code Council. International building code 2006. Country Club Hills, IL: ICC; 2006.
[36] Kramer SL. Geotechnical earthquake engineering. Upper Saddle River, NJ: Prentice Hall; 1996.

[37] Hendry AW. Structural masonry. 2nd ed. London: Macmillan; 1998. https://doi.org/10.1007/978-1-349-14827-1
[38] Agarwal P, Shrikhande M. Earthquake resistant design of structures. New Delhi: PHI Learning; 2008.
[39] Mondal G, Jain SK. Lateral stiffness of masonry infilled reinforced concrete (RC) frames with central opening. Earthquake Spectra. 2008;24(3):701-723. https://doi.org/10.1193/1.2942376
[40] Al-Chaar G. Evaluating strength and stiffness of unreinforced masonry infill structures, ERDC/CERL TR-02-1. Champaign, IL: U.S. Army Corps of Engineers, Engineer Research and Development Center; 2002. https://doi.org/10.21236/ADA407072
[41] Asteris PG, Antoniou ST, Sophianopoulos DS, Chrysostomou CZ. Mathematical macromodeling of infilled frames: state of the art. J Struct Eng. 2011;137(12):1508-1517. https://doi.org/10.1061/(ASCE)ST.1943-541X.0000384
[42] Lysmer J, Kuhlemeyer RL. Finite dynamic model for infinite media. J Eng Mech Div. 1969;95(4):859-877. https://doi.org/10.1061/JMCEA3.0001144
[43] Bureau of Indian Standards. IS 1893 (Part 1): 2016, Criteria for earthquake resistant design of structures, Part 1: General provisions and buildings. New Delhi: BIS; 2016.